Published in final edited form as:
J Am Chem Soc. 2014 January 29; 136(4): 1162–1165. doi:10.1021/ja408513m.

Dynamics of Soft Nanomaterials Captured by Transmission Electron Microscopy in Liquid Water

Maria T. Proetto[1], **Anthony M. Rush**[1], **Miao-Ping Chien**[1], **Patricia Abellan Baeza**[2], **Joseph P. Patterson**[1], **Matthew P. Thompson**[1], **Norman H. Olson**[1], **Curtis E. Moore**[1], **Arnold L. Rheingold**[1], **Christopher Andolina**[3], **Jill Millstone**[3], **Stephen B. Howell**[4], **Nigel D. Browning**[2], **James E. Evans**[5], and **Nathan C. Gianneschi**[*,1]

[1]Department of Chemistry & Biochemistry, University of California, San Diego, La Jolla, CA 92093

[2]Fundamental Computational Sciences Directorate, Pacific Northwest National Laboratory, Richland, WA 99354

[3]Department of Chemistry, University of Pittsburgh, Pittsburgh, PA 15260

[4]Moores Cancer Center, University of California, San Diego, La Jolla CA 92093

[5]Environmental Molecular Sciences Laboratory, Pacific Northwest National Laboratory, Richland, WA 99354

Abstract

In this paper we present *in situ* transmission electron microscopy (TEM) of synthetic polymeric nanoparticles with emphasis on capturing motion in a solvated, aqueous state. The nanoparticles studied were obtained from the direct polymerization of a Pt(II)-containing monomer. The resulting structures provided sufficient contrast for facile imaging *in situ*. We contend that this technique will quickly become essential in the characterization of analogous systems, especially where dynamics are of interest in the solvated state. We describe the preparation of the synthetic micellar nanoparticles together with their characterization and motion in liquid water with comparison to conventional electron microscopy analyses.

Nanoparticles of all types are routinely imaged as static objects by electron microscopy (EM) methods. However, since soft matter is often exclusively composed of elements with low atomic number (Z < 16), image contrast using EM techniques is often low. To resolve soft matter, samples are generally stained using heavy metals or halides. This staining process along with incident high energy electrons can cause damage or physical distortion during the process of characterization itself.[1] Cryo-electron microscopy (cryo-TEM) is sometimes favored because the technique allows materials to be rapidly immobilized in vitreous ice, and hence imaged in what is widely considered a proxy for their native,

Corresponding Author ngianneschi@ucsd.edu.

ASSOCIATED CONTENT

Supporting Information. Detailed materials and sample preparation are included together with additional images and movie files. This material is available free of charge via the Internet at http://pubs.acs.org.

solution phase state. Despite the valuable and complementary information obtained using a combination of these imaging techniques, such an approach is not ideal for the observation of particle dynamics in real-time since either process of drying or freezing completely prohibits native motion. Therefore, a third approach enabling the imaging of synthetic nanoscale particles in their natural, solvated state is necessary and would serve as a complementary method to both dry-state and cryo-TEM. *In situ* liquid TEM, has seen a strong resurgence across many fields including inorganic nanomaterial nucleation and growth from solution,[2–4] electrochemistry[5,6] and biology.[7–9] The first example using an *in situ* liquid environmental holder was demonstrated in 1935.[10,11] However, with the advent of reproducible cryo-TEM,[12] where near-atomic resolution was readily achievable, the use of *in situ* TEM waned. In recent times, advancements in microfabrication techniques and electron microscopy technology including low-dose spherical aberration correction[13] have enabled atomic resolution imaging of immobilized inorganic nanoparticles[2,14] and analyses of their dynamics,[3,15–21] suggesting that *in situ* imaging quality is now limited by the sample instead of the microscope platform. We believe this fact provides a timely opportunity for imaging the dynamics of soft, organic materials on the nanometer length scale. Herein, we describe a pilot study aimed at demonstrating the feasibility of such an imaging strategy for capturing the motion of synthetic soft matter at the nanoscale.

Soft materials are particularly interesting candidates for *in situ* imaging due to the fact that in solution their morphology can be manipulated by a broad range of stimuli[22] including metals,[23] pH,[24] temperature,[25] light,[26] redox chemistry,[27] ultrasound,[28] DNA hybridization,[29] and enzymes.[30] Furthermore, organic liposomes and synthetic polymer vesicles have been imaged *via in situ* TEM as stationary, static objects and structures.[16,31,32] However, to our knowledge there are no examples using this imaging technique to capture the dynamics or motion of soft organic materials at the nanometer length scale. This constitutes a tremendous gap in our capabilities despite the fact that other techniques including dynamic light scattering (DLS), small-angle neutron scattering (SANS), small-angle X-ray scattering (SAXS) and Nanoparticle Tracking Analysis (NTA) are capable of analyzing size and morphology of nanomaterial populations in solution in real time. However, these well-known techniques do not allow for the direct visualization of such changes for individual particles with nanometer resolution.

The studies presented herein were conducted with polymeric micellar nanoparticles obtained from amphiphilic block copolymers in which the hydrophobic block is the result of the direct polymerization of the heavy metal containing norbornyl-monomer which was designed as a square planar Pt(II) complex polymerizable *via* ring-opening metathesis polymerization (ROMP) (Figure 1).[33] The final Pt(II)-core micelles were obtained by dissolving the resulting polymers in DMF, and slowly dialyzing into water over 2 days. DLS and NTA analyses reveal nanoparticles in the 120 nm diameter range (Figures S1–S2, Supporting Information). These systems were chosen for the studies presented here, as micelles loaded with the covalently attached platinum chelate provided exceptional contrast in TEM, eliminating the need for staining during sample preparation (as seen clearly in Figure 1a and Figure S3). In addition, images of unstained particles characterized by STEM-EDS confirm the presence of platinum (Figure 1b, Figures S4–S6).

As an initial demonstration of the power of this technique in imaging soft nanoparticles and their motion in their native solvated state, we present a series of multi-minute movies (see supporting movie files) and corresponding screen shots (Figures 2–3). Single frames of one such movie (Movie_Fig2_Particles_AB.mov and Movie_Fig2_Particles_CDE.mov: see supporting files) are shown in Figure 2, where the motion of the soft nanoparticles in the liquid cell can be clearly observed. Two different particle arrangements captured *in situ* are highlighted: a dimeric and a trimeric species undergoing motion within the field of view. Following particles A and B, we can identify them in contact with each other (red and blue dots indicate particle centers) undergoing varied motion within the imaged field during the time course shown. A similar situation can be observed for particles C, D, and E where the motion of the trimeric system of particles (yellow, pink and green dots indicating particle centers) is greater than that observed for surrounding particles. Time vs. velocity plots clearly demonstrate limited motion for these particles; for example an average velocity of 27 nm/s for particle A is observed. When compared to bulk Brownian motion detected for the same particles by NTA (28,000 nm/s), we conclude that the particles are temporarily adsorbed, but not irreversibly fixed, to the silicon nitride window. Temporal resolution is a key factor when imaging particles in motion, in this experiment a maximum frame rate of 25 frames per second was used, and therefore it would not be possible to observe particles undergoing bulk Brownian motion. Temporal resolution can be greatly improved using dedicated dynamic TEM (DTEM) instruments which have achieved 15 ns frames with 5 nm spatial resolution.[34] However, for standard TEM instruments this is not possible and therefore it is necessary to understand the dynamics of particles in the liquid cell in terms of interactions with the silicon nitride surface, the aqueous solution and with other particles. In the simplest case one can imagine particles undergoing a surface attachment/detachment process whereby particle motion occurs when detached and high-resolution particle observation is possible only when they reattach. This process can be inferred from the velocity ‘jumps’ observed in Figure 2.[21]

In another experiment, to further elucidate these types of dynamic interactions, three particles were tracked within a shorter time frame (Figure 3, Movie_Fig3.mov and for zoom-out and full time course see Movie_S2_Fig3.avi starting at the frame shift at 52 seconds). This tracking analysis reveals concerted motion between the three particles. It is interesting to note that these particles seem to undergo cooperative motion. This could be due to beam induced charging effects between particles, charging effects induced from solution, or charging effects from the silicon nitride surface itself. It appears that these sorts of coulombic interactions operate on the second to minute time scale. Recognizing and controlling these types of interactions will be of crucial importance in developing *in situ* imaging of nanomaterials in the immediate future. Furthermore, radiolysis from the electron beam plays a key role in the behavior of materials inside the imaging cell itself.[35] Understanding the rate and impact of this type of damage will be key in developing new design parameters for these types of analyses. In this instance, micellar nanoparticles appear to be physically stable against electron beam damage for several minutes, after which the particles appear to agglomerate. This suggests that time-resolved observations of organic nanoparticles undergoing stimuli responsive dynamics on the seconds to minutes time scale should be possible. Therefore, the study presented herein serves as a necessary part of

ongoing work to determine the threshold under which imaging experiments can be used to glean meaningful information for soft materials and their dynamics.

Having analyzed particle dynamics via *in situ* TEM, we sought to compare observed morphologies with standard and cryogenic TEM methods. Therefore, the materials were characterized by dry-state TEM without stain (Figure 1 and Figure S8) and with uranyl acetate staining (Figure S9). Furthermore, cryo-TEM, similar to observations for *in situ* and unstained TEM experiments, reveals high contrast for this class of particle (Figure 4 and Figure S10). Image analysis of particles (Figures S8–S11) shows a small variation in size but overall we observed Gaussian fits for each technique showing maximum intensities centered at approximately 90 nm (see Figure S12). *In situ* measurements reveal what appears to be a tighter distribution of sizes, however, analyses of *in situ* samples were only conducted on particles that were obviously spherical from snapshots, limiting the population size that could be analyzed in this initial study. It is important to note this as it highlights an inherent feature of the approach, namely, that multiple particles can occupy a similar position within the field of view but differ with respect to the vertical axis through the sample and therefore may appear as aggregates (Figure 4). This is clearly observed in movies that reveal sets of particles passing over each other in solution confirming they are separate species overlayed in the z-axis; for example, this is clearly observed in Figure 2, particles A and B. From these parallel analyses we can conclude that *in situ* TEM is capable of capturing soft nanoparticle morphologies in a manner comparable to more traditional techniques, with the added capability of allowing one to image particles in motion.

In summary, we have demonstrated that *in situ* TEM is a viable approach for imaging the motion of organic, polymeric soft nanomaterials in liquid water. In terms of soft materials, *in situ* TEM should become a new standard to add to the suite of microscopy methods employed to interrogate structure. Furthermore, with an understanding of operational parameters and limitations of the materials in hand, the technique should prove to become a unique tool for high resolution characterization of *dynamic* systems. Finally, we note that these particles, loaded with a heavy metal for contrast, made for an initial, straightforward imaging study *in situ*. However, we do not believe that this heavy metal loading strategy is a prerequisite, and are currently screening other organic materials and dynamic, switchable systems for their ability to be imaged. These studies are currently underway and we aim to describe these in due course.

Supplementary Material

Refer to Web version on PubMed Central for supplementary material.

Acknowledgments

We acknowledge support for this work from the AFOSR via a PECASE (FA9550-11-1-0105), AFOSR (FA9550-12-1-0414), ARO (W911NF-11-1-0264) and from the NIH (NIBIB - R01EB011633) and NIH New Innovator (DP2OD008724). M.T.P. thanks the UCSD Cancer Researchers in Nanotechnology for a postdoctoral fellowship, and the mentorship of Prof Andrew Kummel (UCSD) within that program. A portion of this work was performed using EMSL, a national scientific user facility sponsored by the Department of Energy's Office of Biological and Environmental Research and located at Pacific Northwest National Laboratory. Pacific Northwest National Laboratory is operated by Battelle Memorial Institute for the U.S. Department of Energy under Contract No. DE-AC05-76RL01830. We acknowledge use of the UCSD Cryo-Electron Microscopy Facility, which is

supported by NIH grants to Dr. Timothy S. Baker and a gift from the Agouron Institute to UCSD. M.T.P. thanks Dr. Dariusz Stramski and Jan Tatarkiewicz from Scripps Institution of Oceanography, UCSD for making available NanoSight instrument and assistance during experiments.

References

1. Egerton RF. Ultramicroscopy. 2013; 127:100–8. [PubMed: 22910614]
2. Evans JE, Jungjohann KL, Browning ND, Arslan I. Nano Lett. 2011; 11:2809–13. [PubMed: 21619024]
3. Woehl TJ, Evans JE, Arslan I, Ristenpart WD, Browning ND. ACS Nano. 2012; 10:8599–610. [PubMed: 22957797]
4. Zheng H, Smith RK, Jun YW, Kisielowski C, Dahmen U, Alivisatos AP. Science. 2009; 324:1309–12. [PubMed: 19498166]
5. Williamson MJ, Tromp RM, Vereecken PM, Hull R, Ross FM. Nat Mater. 2003; 2:532–6. [PubMed: 12872162]
6. White ER, Singer SB, Augustyn V, Hubbard WA, Mecklenburg M, Dunn B, Regan BC. ACS Nano. 2012; 6:6308–17. [PubMed: 22702348]
7. Sugi H, Minoda H, Inayoshi Y, Yumoto F, Miyakawa T, Miyauchi Y, Tanokura M, Akimoto T, Kobayashi T, Chaen S, Sugiura S. Proc Natl Acad Sci USA. 2008; 105:17396–401. [PubMed: 18987316]
8. Peckys DB, Veith GM, Joy DC, de Jonge N. PLoS One. 2009; 4:e8214. [PubMed: 20020038]
9. Evans JE, Jungjohann KL, Wong PC, Chiu PL, Dutrow GH, Arslan I, Browning ND. Micron. 2012; 43:1085–90. [PubMed: 22386621]
10. Marton L. Bull Acad Roy Med Belg. 1935; 21:600–17.
11. Parsons DF. Science. 1974; 186:407–14. [PubMed: 4213401]
12. Adrian M, Dubochet J, Lepault J, McDowall AW. Nature. 1984; 308:32–6. [PubMed: 6322001]
13. Evans JE, Hetherington C, Kirkland A, Chang LY, Stahlberg H, Browning N. Ultramicroscopy. 2008; 108:1636–44. [PubMed: 18703285]
14. Jungjohann KL, Evans JE, Aguiar JA, Arslan I, Browning ND. Microsc Microanal. 2012; 18:621–7. [PubMed: 22640968]
15. Liao HG, Zheng HM. J Am Chem Soc. 135:5038–43. [PubMed: 23477794]
16. Mueller C, Harb M, Dwyer JR, Miller RJD. J Phys Chem Lett. 2013; 4:2339–47.
17. Yuk JM, Park J, Ercius P, Kim K, Hellebusch DJ, Crommie MF, Lee JY, Zettl A, Alivisatos AP. Science. 2012; 336:61–4. [PubMed: 22491849]
18. Liao HG, Cui LK, Whitelam S, Zheng HM. Science. 2012; 336:1011–4. [PubMed: 22628649]
19. Li DS, Nielsen MH, Lee JRI, Frandsen C, Banfield JF, De Yoreo JJ. Science. 2012; 336:1014–8. [PubMed: 22628650]
20. Chen Q, Smith JM, Park J, Kim K, Ho D, Rasool HI, Zettl A, Alivisatos AP. Nano Lett. 2013; 13:4556–61. [PubMed: 23944844]
21. Zheng HM, Claridge SA, Minor AM, Alivisatos AP, Dahmen U. Nano Lett. 2009; 9:2460–5. [PubMed: 19408927]
22. Kelley EG, Albert JNL, Sullivan MO, Epps TH III. Chem Soc Rev. 2013; 42:7057–71. [PubMed: 23403471]
23. Brodin JD, Ambroggio XI, Tang C, Parent KN, Baker TS, Tezcan FA. Nat Chem. 2012; 4:375–82. [PubMed: 22522257]
24. Doncom KEB, Hansell CF, Theato P, O'Reilly RK. Polym Chem. 2012; 3:3007–15.
25. Xing Z, Zhang J, Li X, Zhang W, Wang L, Zhou N, Zhu X. J Polym Sci A1. 2013; 51:4021–30.
26. Jiang J, Tong X, Zhao Y. J Am Chem Soc. 2005; 127:8290–1. [PubMed: 15941255]
27. Ren H, Wu Y, Ma N, Xu H, Zhang X. Soft Matter. 2012; 8:1460–6.
28. Lensen D, Gelderblom EC, Vriezema DM, Marmottant P, Verdonschot N, Versluis M, de Jong N, van Hest JCM. Soft Matter. 2011; 7:5417–22.
29. Chien MP, Rush AM, Thompson MP, Gianneschi NC. Angew Chem, Int Ed. 2010; 49:5076–80.

30. Ku TH, Chien MP, Thompson MP, Sinkovits RS, Olson NH, Baker TS, Gianneschi NC. J Am Chem Soc. 2011; 133:8392–5. [PubMed: 21462979]

31. Hoppe SM, Sasaki DY, Kinghorn AN, Hattar K. Langmuir. 2013; 29:9958–61. [PubMed: 23886420]

32. Plamper FA, Gelissen AP, Timper J, Wolf A, Zezin AB, Richtering W, Tenhu H, Simon U, Mayer J, Borisov OV, Pergushov DV. Macromol Rapid Comm. 2013; 34:855–60.

33. Xia Y, Olsen BD, Kornfield JA, Grubbs RH. J Am Chem Soc. 2009; 131:18525–32. [PubMed: 19947607]

34. LaGrange T, Campbell GH, Reed BW, Taheri M, Pesavento JB, Kim JS, Browning ND. Ultramicroscopy. 2008; 108:1441–9. [PubMed: 18783886]

35. White ER, Mecklenburg M, Shevitski B, Singer SB, Regan BC. Langmuir. 2012; 28:3695–8. [PubMed: 22320230]

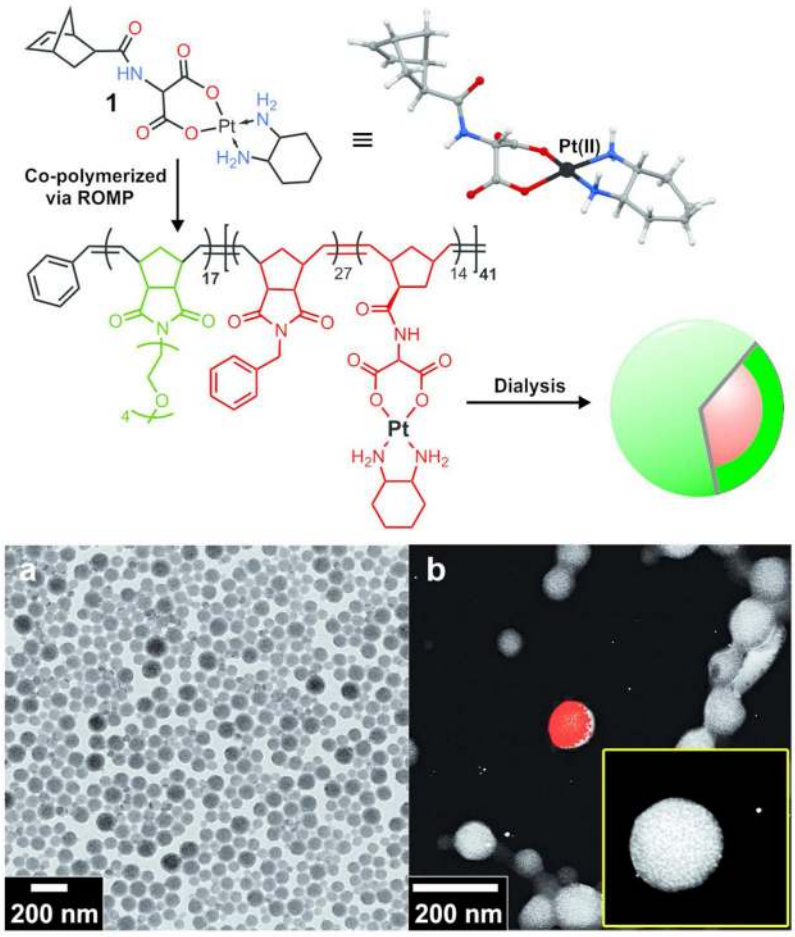

Figure 1.

Preparation of micellar nanoparticles consisting of a Pt(II)-labeled core. TOP: Structure of Pt(II)-nobornyl monomer (**1**), X-ray crystal structure and amphiphilic block copolymer. Dialysis from DMF into water yielded high contrast, spherical micelles with Pt(II)-labeled cores (red). BOTTOM: a) Conventional dry-state TEM of unstained micelles. b) STEM-energy-dispersive X-ray spectroscopy (STEM-EDS) elemental map indicating platinum overlaid on the corresponding STEM-High-angle annular dark-field microscopy (HAADF) image. Inset shows zoomed STEM-HAADF image of a particle (yellow box has horizontal dimension of 200 nm).

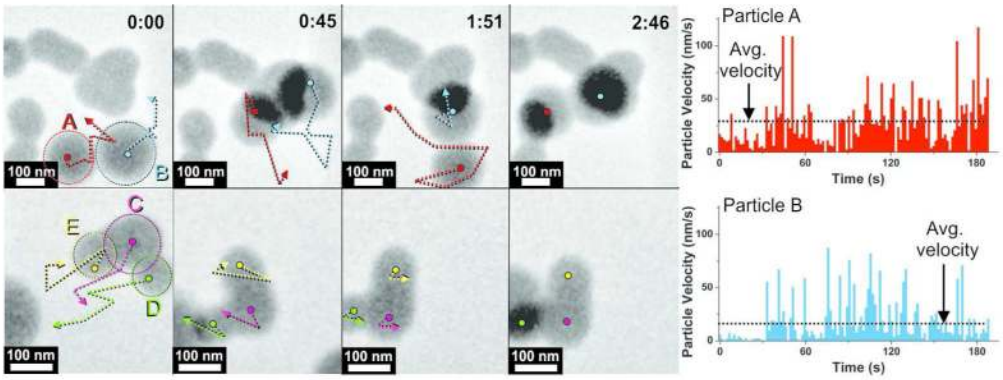

Figure 2.

LEFT Frames: Sequential snapshots from *in situ* TEM movies of nanoparticles in liquid water at times shown. Five particle centers (A–E) where selected with arrows indicating particle motion during the time lapse. RIGHT: Velocity vs. time plots for particles A and B highlighting distinct motion for each of the two connected particles. The dotted line in each graph represents the average velocity for each particle during the imaged time lapse (Average velocity, particle A = 27.5 nm/s, particle B = 18.0 nm/s). See Figure S7, Supporting Information for velocity plots for particles C, D, and E. Time displayed as minutes:seconds in movie frames. Motion and velocity analyses were performed using ImageJ with MTrackJ plugin. For movies see supporting files: Movie_Fig2_Particles_AB.mov, Movie_Fig2_Particles_CDE.mov, and Movie_S1_Fig2.avi. Images captured in silicon nitride *in situ* cells with 50 nm thick windows.

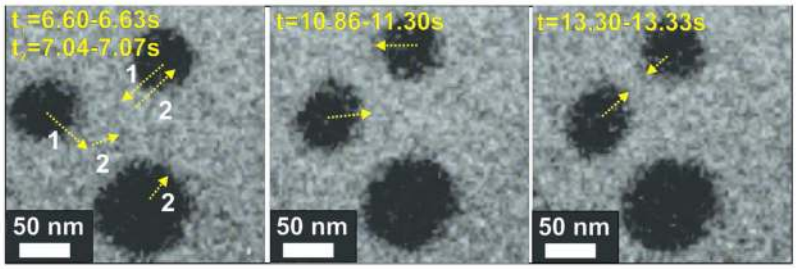

Figure 3.

Screen shots from an *in situ* liquid stage movie. Arrows indicate direction of motion between the times indicated (see Movie_Fig3.mov). Time is displayed in seconds.

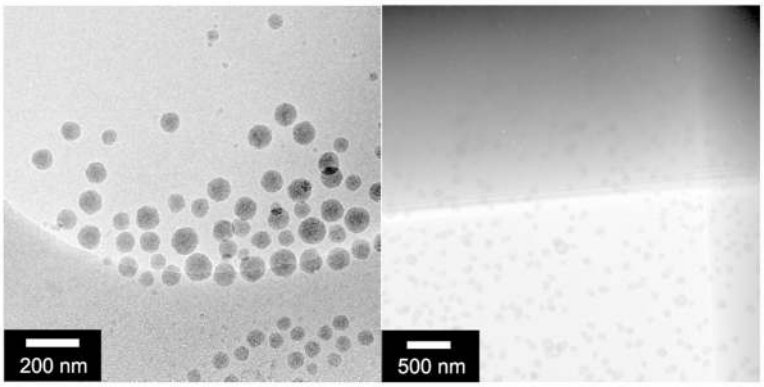

Figure 4.
Comparison of Pt(II)-core micelles visualized via cryo- (left) and *in situ* (right) TEM showing dispersed particles for each method.